Journal of Nanophotonics

Nanophotonics.SPIEDigitalLibrary.org

Advances in nonlinear optical microscopy for biophotonics

Rui Li
Xinxin Wang
Yi Zhou
Huan Zong
Maodu Chen
Mengtao Sun

SPIE.

Rui Li, Xinxin Wang, Yi Zhou, Huan Zong, Maodu Chen, Mengtao Sun, "Advances in nonlinear optical microscopy for biophotonics," *J. Nanophoton.* **12**(3), 033007 (2018), doi: 10.1117/1.JNP.12.033007.

REVIEW

Advances in nonlinear optical microscopy for biophotonics

Rui Li,[a,†] Xinxin Wang,[b,†] Yi Zhou,[a] Huan Zong,[b] Maodu Chen,[a,*] and Mengtao Sun[a,b,*]

[a]Dalian University of Technology, School of Physics, Dalian, China
[b]University of Science and Technology Beijing, School of Mathematics and Physics, Center for green Innovation, Beijing Key Laboratory for Magneto-Photoelectrical Composite and Interface Science, Beijing, China

Abstract. This article reviews recent advances in nonlinear optical microscopy for biophotonics, including stimulated Raman scattering (SRS), coherent anti-Stokes Raman scattering (CARS), two-photon excited fluorescence (TPEF), second harmonic generation (SHG), and sum frequency generation (SFG). We first introduce the principles and applications of SRS, CARS, TPEF, SHG, and SFG and their individual applications for biophotonics. We then introduce the combination of SRS, CARS, TPEF, SHG, and SFG microscopy for biophotonics. Our review not only summarizes the recent advances in nonlinear optical microscopy but also can deepen the understanding of the combination of these types of nonlinear optical microscopy for biophotonics. © *2018 Society of Photo-Optical Instrumentation Engineers (SPIE)* [DOI: 10.1117/1.JNP.12.033007]

Keywords: nonlinear optical microscopy; biophotonics; stimulated Raman scatting; coherent anti-Stokes Raman scattering; two-photon excited fluorescence; second harmonic generation; sum frequency generation.

Paper 18100SSV received Jun. 6, 2018; accepted for publication Jul. 30, 2018; published online Aug. 14, 2018.

1 Introduction

Over the past decade, the nonlinear optical methods have become widely used tools for biomolecular detection, medical diagnosis in cells or tissues at the micrometer and nanometer level.[1] Advancement of these optical methods promotes and enhances basic research in biology, pharmacy, and medicine.[2–4] Compared with the optical method, radiation is usually applied for imaging modalities, including x-rays, computed tomography, plain radiography, magnetic resonance imaging, and other nuclear imaging methods.[5] However, these techniques are costly and emit radiation. For disease detection and diagnoses and cells development process, optical imaging methods can provide molecular information on human tissues with noninvasive, real-time, accurate, sensitive, and economic properties, as discussed in recent reviews.[6] When human diseases develop, cells and tissues are used to study the genetics, drug screening, and disease control via optical imaging techniques.[7–9] Among optical imaging technologies, the nonlinear optical methods have great advantages such as noninvasiveness, depth penetration, high sensitivity, and ultrahigh resolution. The nonlinear signal is generated via nonlinear optical microscopy in a small area (measured in nanometers) in the focal plane of the objective lens using a pico- or femtosecond near-infrared pulsed excited laser. This technology noninvasively enables tissue depth penetration, image sensitivity, and high resolution, as discussed in recent reviews.[10–12]

Combined various fluorescent dye labels[13,14] and two-photon excited fluorescence (TPEF) microscopy are potentially used in laboratories and clinics to analyze live cells and accurately

*Address all correspondence to: Mengtao Sun, E-mail: mengtaosun@ustb.edu.cn; Maodu Chen, E-mail: mdchen@dlut.edu.cn
†Equal Contribution

1934-2608/2018/$25.00 © 2018 SPIE

Table 1 Representative example applications of nonlinear optical microscopy.

Nonlinear optics method	Tissues or cells
TPEF	Ovarian cancer[25]
	Brain[8,21]
	Mouse L929 fibroblastic[7]
	Mouse sciatic nerve[26]
	Mouse living[27]
	Axonal myelin[28]
	Neonatal cardiomyocyte[23,29]
	HeLa cells[22]
	C. elegans[9]
	Oocyte, embryo, egg[4]
CARS	Brain[8,21]
	Mouse L929 fibroblastic[7]
	C. elegans[9]
	Axonal myelin[28]
	Oocyte, embryo, egg[4]
	Human stem cells[30]
	Human mastoid cortex[11]
	Breast and prostate cancer cells[31]
SRS	Brain[16,20]
	Mouse sciatic nerve[26]
	Human lung cancer cells[32]
	C. elegans[33]
	Mouse skin[32]
	HeLa cells[22]
	Human macrophages[34]
SHG	Neonatal cardiomyocyte[29,33]
	Human mastoid cortex[11]
	Cardiac myocytes[23]
SFG	*C. elegans*[24]

localize and completely resect live tumors.[15] Live cells and tissues also can be imaged without external labeling by directly tracking different chemical bonds or proteins with nonlinear optical microscopes such as stimulated Raman scatting (SRS),[16–19] coherent anti-Stokes Raman scattering (CARS), TPEF, second harmonic generation (SHG), and sum frequency generation (SFG), among other techniques.

In this review, we will discuss several nonlinear methods began to be used in cells and tissues optics, such as SRS,[16,20] CARS,[8,21] TPEF,[22] SHG,[23] SFG,[24] and multiple combinations of techniques. Although it is not comprehensive, an overview of nonlinear optics method applications with representative references is given in Table 1.

2 Single Experimental Methods

In both nonlinear microscopy and confocal laser scanning microscopy, a vibrating mirror scans the sample with focused laser beams.[35] In confocal laser scanning microscopy, a high-resolution optical sectioning image is obtained with pinhole apertures.

In biology and medicine, optical microscopy is restricted by phototoxicity. Each measurement often necessitates the minimum average energy of an excited laser to avoid phototoxicity. Compared to linear processes, nonlinear processes can provide momentary extremely high pulsed excited light with low average energy on a live sample. Near-infrared excitation light is typically used in nonlinear excitation microscopy and can also decrease the phototoxicity. Using infrared light can minimize scattering in live cells and tissues. All of these effects increase the penetration depth of nonlinear microscopes.

The technology and theories of nonlinear optical microscopy have made significant contributions to biological research and medical diagnoses.[36] The potential applications of these nonlinear optical microscopes are in the fields of biology and medicine. An energy-level diagram of a variety of nonlinear optical processes, including TPEF, SHG, SFG, CARS, and SRS, is shown in Fig. 1.

To accurately study nonlinear optical microscopy, the relationship between polarization $\mathbf{P}(t)$ and electric field strength is used to precisely describe nonlinear optical microscopy using the following equation:[37]

$$\mathbf{P}(\mathrm{t}) = \varepsilon_0[\chi^{(1)}\mathbf{E}(\mathrm{t}) + \chi^{(2)}\mathbf{E}^2(\mathrm{t}) + \chi^{(3)}\mathbf{E}^3(\mathrm{t}) + \ldots], \tag{1}$$

where $\chi^{(1)}$, $\chi^{(2)}$, and $\chi^{(2)}$ are the linear, second-order, and third-order susceptibility, respectively. ε_0 is the permittivity of free space. The second-order nonlinear optics are described using the following equation:[37]

$$\mathbf{P}(\omega_1 + \omega_2) = 2\varepsilon_0\chi^{(2)}\mathbf{E}_1\mathbf{E}_2. \tag{2}$$

SHG and SFG are labeled as $\omega_1 = \omega_2$ and $\omega_1 \neq \omega_2$.

The third-order nonlinear optics (CARS and SRS) are described using the following equations:[37]

$$\mathbf{P}(\omega_1 + \omega_2 - \omega_3) = 6\varepsilon_0\chi^{(3)}\mathbf{E}_1\mathbf{E}_2\mathbf{E}_3^*, \tag{3}$$

$$\mathbf{P}(2\omega_1 - \omega_2) = 3\varepsilon_0\chi^{(3)}\mathbf{E}_1^2\mathbf{E}_2^*. \tag{4}$$

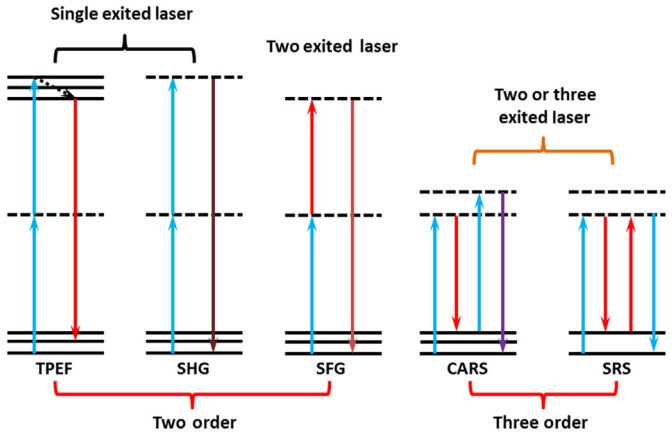

Fig. 1 Energy-level diagram for nonlinear optical processes of TPEF, SHG, SFG, CARS, and SRS process.

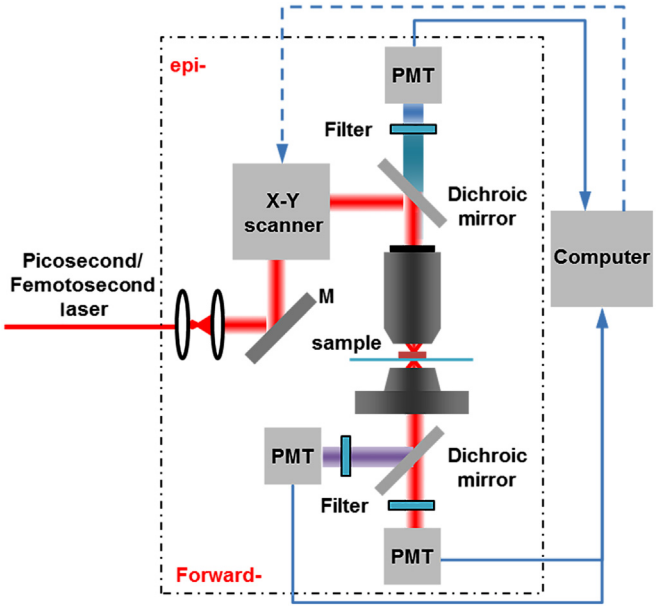

Fig. 2 Diagram of a TPEF or SHG microscope with epi and forward channel.

2.1 *Two-Photon Excited Fluorescence*

TPEF microscopy is one of the traditional fluorescence imaging techniques. Due to its nonlinear optical effects, the penetration depth can reach 1 mm in live tissue with high resolution and high sensitivity. Combining TPEF microscopy with fluorescence materials can provide rapid techniques to diagnose and monitor a variety of diseases using encoded fluorescent proteins, exogenous dyes, and nanomaterials.[25] A picosecond or femtosecond beam is focused on the sample using a scanning microscope to generate a fluorescence signal (Fig. 2). TPEF microscopy uses exogenous markers to detect and diagnose live cancer cells' phenotypic changes, metabolic activity, and protein expression.[38] Live ovarian cancer cells have been studied using TPEF microscopy to detect β-galactosidase with lysosome-targetable and two-photon fluorescent probe FC-βgal, which are important for the diagnosis of primary ovarian cancer (Fig. 3).[25]

2.2 *Second-Harmonic Generation*

In general, for the second-order nonlinear optical techniques of three-wave mixing, the generation of a w3 photo has to emit one w1 and one w2 photon (w1 + w2 = w3). When w1 equals w2, it is defined as SHG (Fig. 1); otherwise, it is defined as SFG (Fig. 1).[39] SHG occurs when an incident laser beam passes through a noncentrosymmetric and highly ordered medium such as tendons, axons, and striated muscle. Due to the nonabsorptive effects of nonlinear processes, SHG inhibits photobleaching.[40] SHG was discovered by Franken in 1961.[41] Because it uses the same laser scanning microscope and laser source with an additional proper narrow band filter, SHG can be combined with other nonlinear equipment. SHG is suitable for the collagen, microtubules, and muscles in live tissues and cells[42] and is widely applied for biological research, medical diagnoses,[43] and medicine.[10,29,23,42,44] SHG microscopy has been used to measure the muscles' contractile integrity via sarcomeric myosin imaging. Previous studies found that the muscle contractile integrity and neuromuscular health are strongly correlated in mice (Fig. 4).[44]

2.3 *Coherent Anti-Stokes Raman Scattering*

CARS is one of the most powerful Raman techniques for imaging molecular vibrations in live cells and tissues as discussed in recent reviews.[3,45,46–50] Similar to SRS, CARS is also generated

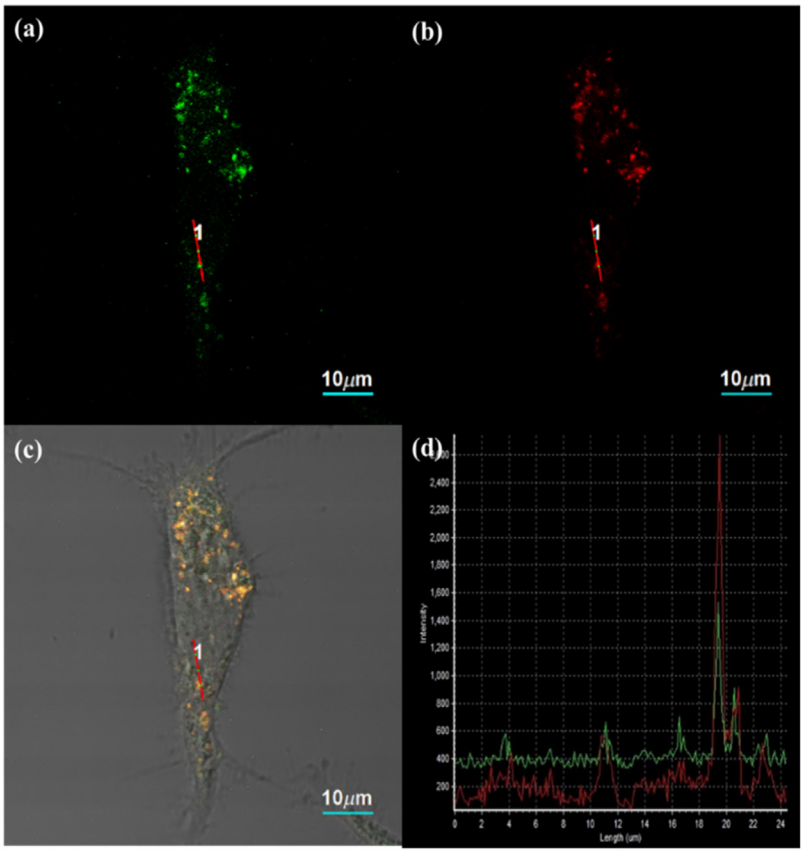

Fig. 3 TPEF images of living ovarian cancer SKOV-3cells, (a) probe FC-βgal image of β-gal, (b) probe lysosome image of LysoTracker Red DND-99 by the tracker, (c) merged image of (a) and (b), and (d) intensity profile of regions of interest across SKOV-3 cells, adapted from Ref. 25.

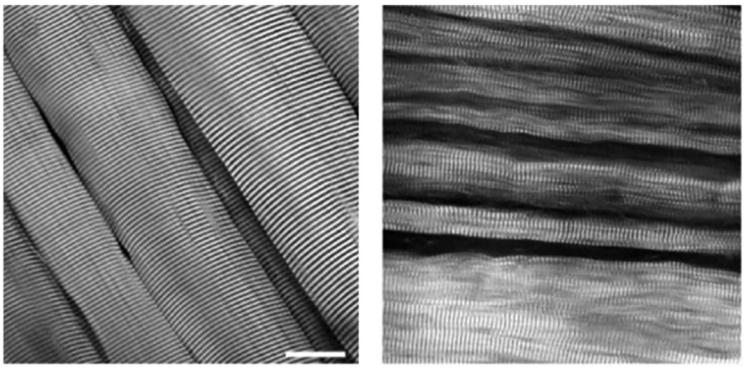

Fig. 4 SHG images of normal and diseased gastrocnemius muscle dissected, (a) normal muscle and (b) diseased muscle, adapted from Ref. 44.

by four-wave mixing with a three-order nonlinear effect, and these work together in the same process. However, unlike SRS, anti-Stokes signal is used for molecular imaging, and a variation in the pump intensity is applied in SRS microscopy.[51] Collinear picosecond or femtosecond beams (pump and Stokes) are focused on the sample using a scanning microscope to generate anti-Stokes signals (Fig. 5). Similar to SRS, CARS microscopy is widely applied for imaging

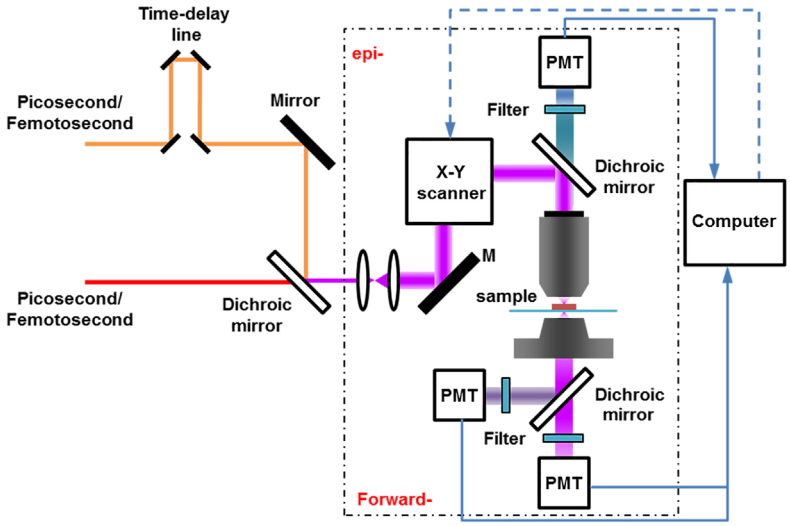

Fig. 5 Diagram of a CARS or SFG microscope with epi and forward channel.

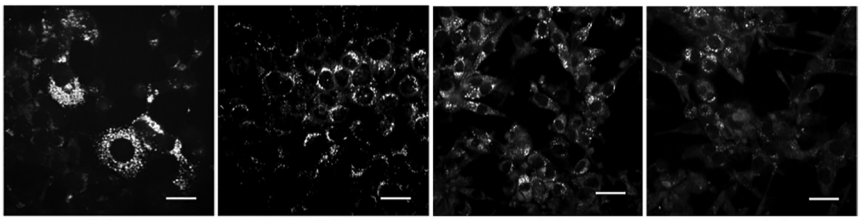

Fig. 6 CARS images of treated versus vehicle control living breast and prostate cancer cells. (a) Medroxyprogesterone acetate treated and (b) untreated breast cells, (c) synthetic androgen R1881treated, and (d) untreated prostate cells, scale bar 30 μm, adapted from Ref. 52.

live cancer cells,[31,52] probing the interactions between live cells and plasmas,[53] investigating intracellular lipid storage and dynamics in live tissues,[54] and assessing lipid uptake in live stem cells during differentiation,[30] with the same source, ease of use, real-time, label-free, and ultrahigh resolution. CARS is used to image lipids and measure their number and size to analyze their effects on hormone-treated breast and prostate cancer cells as shown in Fig. 6.

2.4 *Stimulated Raman Scattering*

SRS is a form of Raman scattering. Similar to Raman, it uses femtosecond or picosecond lasers to directly image the vibrational fingerprints of live cells and tissues. SRS is also a special case of four-wave mixing with the three-order nonlinear effect. SRS can provide high-speed, ultrahigh resolution, high-sensitivity, free label, real-time, and three-dimensional[55] properties to image the distribution of specific molecules[56] and monitor glucose metabolic activity,[2] intracellular drug uptake,[19,32,57,58] and image the vibration of newly synthesized proteins,[18,59] image multiple proteins *in situ*,[16,60,61] detect brain tumors,[20] and probe the interactions between nanoparticles and live cancer cells.[62] Based on the configuration of CARS microscopy, electro-optical modulators or acousto-optic modulators and lock-in amplifiers are added to the Stokes beam and photomultiplier tube, respectively, to generate an SRS signal (Fig. 7). Macrophages are among the most important white blood cells in the immune systems of animals. They phagocytose cancer cells and cell debris, among other functions. SRS microscopy was first used to characterize the different uptake kinetics of d31-palmitic acid by macrophages between individual cells as shown in Fig. 8.

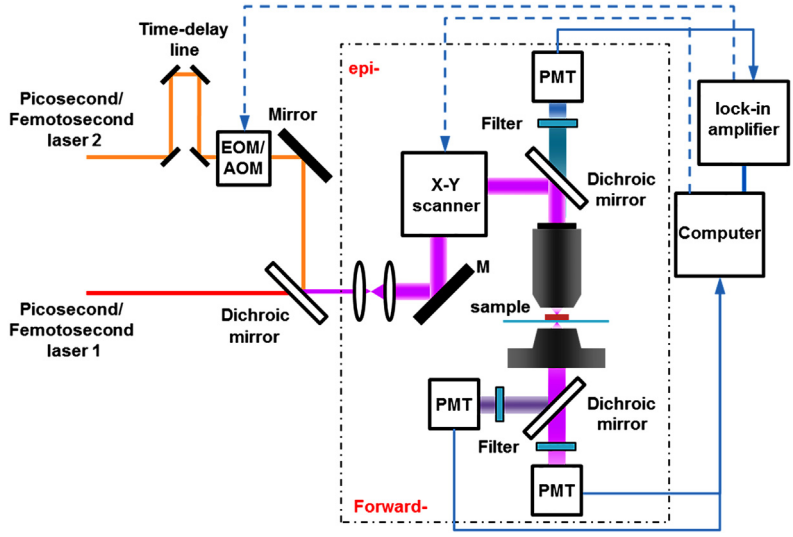

Fig. 7 Diagram of an SRS microscope with epi and forward channel.

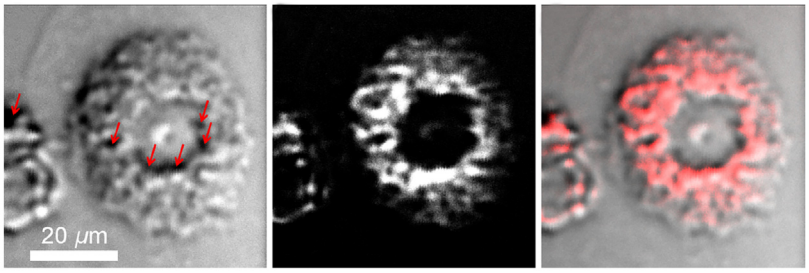

Fig. 8 SRS image of a fixed living human macrophage cells in d31-palmitic acid environment with the corresponding Raman shift being 2125 cm^{-1}. (a) Nonresonant background of CARS signal, (b) SRS image, (c) merge image of SRS (red), and CARS (gray), adapted from Ref. 34.

3 Multiple Experimental Methods

Picosecond or femtosecond pulsed laser and multi- or two-photon scanning microscopes are used in SRS and CARS. Many useful signals can be applied to biological research and medical diagnosis, such as TPEF, SHG, and SFG.

3.1 *Two Methods*

3.1.1 *TPEF and SHG*

Both TPEF and SHG are second-order nonlinear processes with minimum device, single incident lasers, and the same optical system.[10,29,23] The distribution of alpha-actinin with fluorescence drugs and sarcomeric structures in live embryonic cardiomyocytes is imaged using TPEF and SHG channels, respectively. This second-order nonlinear optical technique can effectively reveal long-term structural changes in the live DiO-stained myofibrillogenesis of a single cardiomyocyte using real-time, high-resolution, and high-speed (4 SPF) features as shown in Fig. 9.

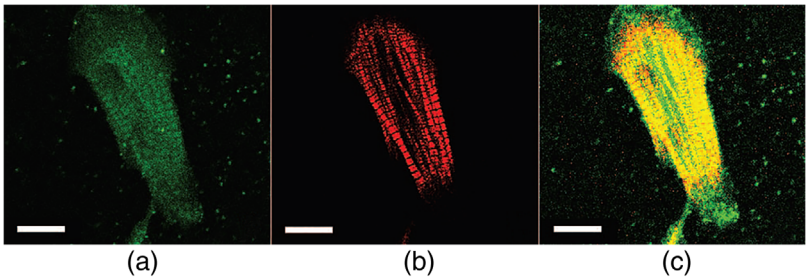

Fig. 9 TPEF and SHG images of living cultured neonatal cardiomyocyte: (a) TPEF image, (b) SHG image of sarcomeric structure, and (c) merged of images (scale bars: 10 μm), adapted from Ref. 29.

3.1.2 *SRS and TPEF*

TPEF and SRS microscopy are combined with new features to image live cells and tissues. They can provide similar quality images with the same organelles of live cells as shown in Fig. 10.[22] Deferent organelles can also be imaged using TPEF and SRS, respectively. In a recent study, the distribution of lipid droplets and the endoplasmic reticulum was obtained in cancer cells *in situ*. The spatial–temporal dynamics of lipid droplets and the endoplasmic reticulum in live cancer cells can be monitored to study organelle dynamics and metabolism as shown in Fig. 10(d).[63]

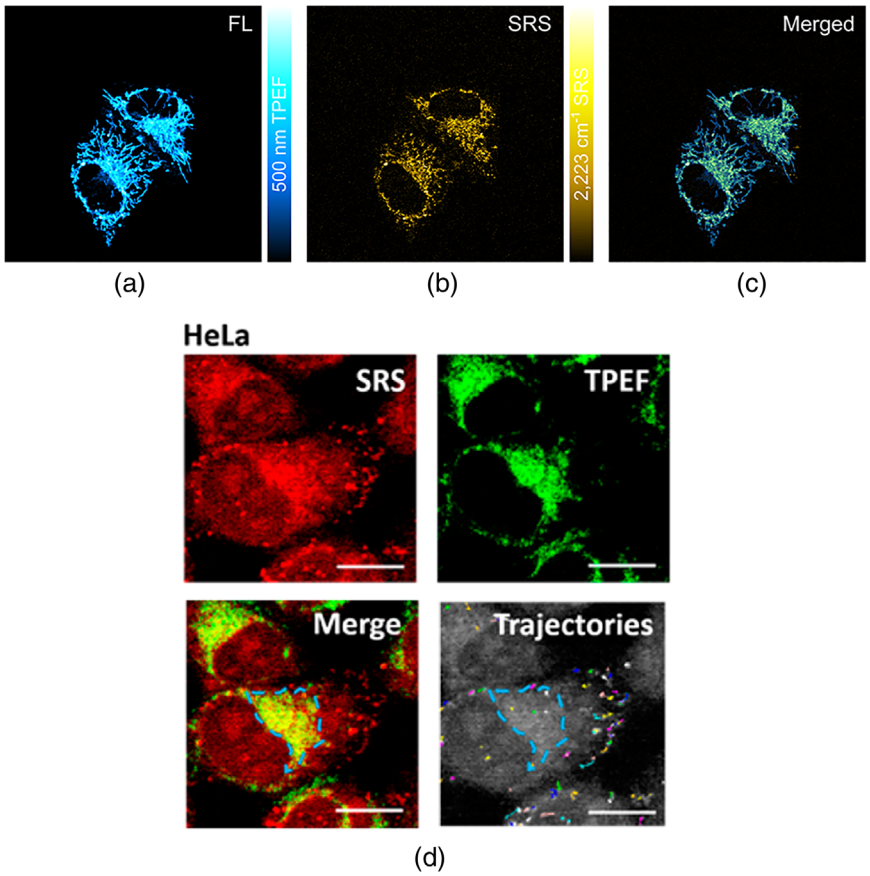

Fig. 10 (a) TPEF image, (b) SRS image, and (c) merged image of living Hela cancer cells, adapted from Ref. 22. (d) SRS, TPEF, merged, and trajectories images of living Hela cancer cells, adapted from Ref. 63.

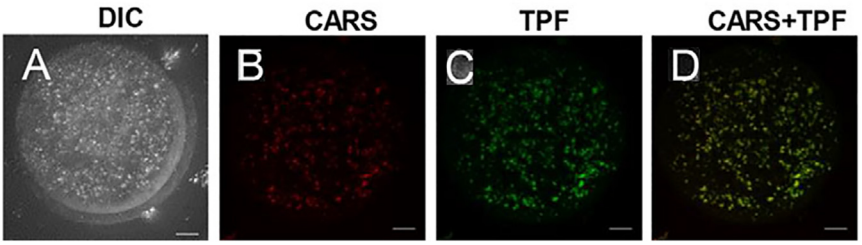

Fig. 11 (a) DIC, (b) CARS, (c) TPEF, and (d) merged images in living early embryonic stages. The CARS images are shown with the corresponding Raman shift being 2850 cm^{-1}, adapted from Ref. 4.

3.1.3 *CARS and TPEF*

Due to the spectra overlap of TPEF and CARS signals, they cannot be easily separated. Using the correct wavelength of the pump and probe source solves this problem. As female gametocytes and germ cells are involved in reproduction, oocytes are the earliest stages of mammals. As with early embryos, they are widely used to study genetic diseases, cloned animals, genetic breeding, organ transplantation, and cell differentiation mechanisms. Lipid droplets store fatty acids and play a significant role in the preimplantation development of oocytes. Combined CARS and differential interference contrast (DIC) microscopy have been used to quantitatively image lipids in live mouse oocytes and early embryos at different stages of cell division as shown in Fig. 11.

3.1.4 *CARS and SHG*

Stem cell-based bone engineering is a treatment for bone regeneration. Combined CARS and SHG microscopy has been used to image the apatite and collagen of live cells, respectively, as shown in Fig. 12.[11]

3.2 *Three Methods*

With the appropriate filters, fluorescent labels, and excited wavelengths, three or more types of nonlinear optic microscopy can be combined in the same scanning microscope. The results indicate that these multiple processes are advantageous for imaging live tissues or animals.[7,24] *Caenorhabditis elegans*, a free-living (nonparasitic) transparent nematode (roundworm) ~1 mm in length, is widely used in genetics and developmental biology, behavior and neurobiology, aging and longevity, human genetic diseases, pathogen and biological interactions, drug screening, animal emergency response, and other fields. CARS, SFG, and TPEF have been used to study the muscle of live *C. elegans* using a scanning microscope with an excited laser as shown in Fig. 13.

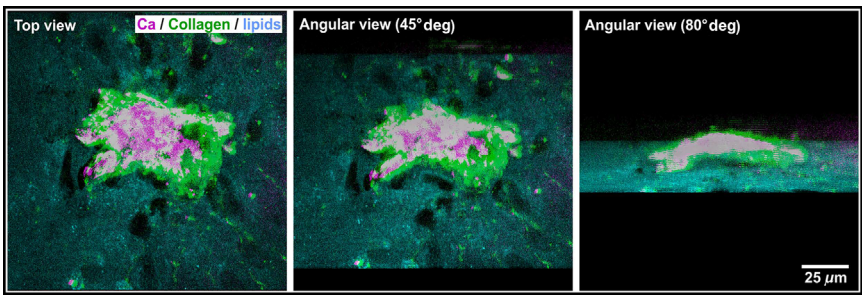

Fig. 12 CARS (magenta) and SHG (green) three-dimensionality images of calcium hydroxyapatite deposits embedded in collagen. The SHG image of collagen is shown with 532 nm, adapted from Ref. 11.

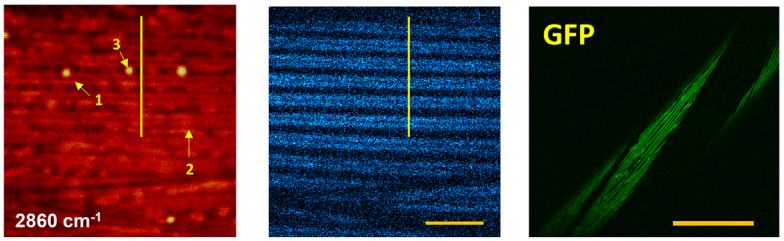

Fig. 13 (a) CARS (Red), (b) SFG (Blue), and (c) TPEF (green fuorescent protein, Green) images of muscle of *C. elegans* for the 2860 cm^{-1} vibration mode. Scale bar is 10 and 50 μm, adapted from Ref. 24.

4 Conclusion

We have summarized the principles, applications, and advantages of individual and combination of several types of nonlinear optical microscopy, including SRS, TPEF, SHG, and SFG. The experimental results indicate that these multiple processes are of great advantage for imaging live tissues or animals, *C. elegans*. The nonlinear optical microscopy can monitor specific molecules and proteins inside cells and tissues in three dimensions with high sensitivity and ultrahigh resolution. Our review can promote further understanding of the advanced application of combination of these types of nonlinear optical microscopy for biophotonics.

Acknowledgments

This work was supported by the National Natural Science Foundation of China (Grant Nos. 91436102, 11374353, 11474141, 51401239, and 11704058), Fundamental Research Funds for the Central Universities in USTB, and National Basic Research Program of China (Grant No. 2016YFA0200802).

References

1. L. Opilik, T. Schmid, and R. Zenobi, "Modern Raman imaging: vibrational spectroscopy on the micrometer and nanometer scales," *Annu. Rev. Anal. Chem.* **6**(1), 379–398 (2013).
2. W. Hong et al., "Antibiotic susceptibility determination within one cell cycle at single-bacterium level by stimulated Raman metabolic imaging," *Anal. Chem.* **90**, 3737–3743 (2018).
3. R. E. Kast et al., "Emerging technology: applications of Raman spectroscopy for prostate cancer," *Cancer Metastasis Rev.* **33**(2), 673–693 (2014).
4. J. Bradley et al., "Quantitative imaging of lipids in live mouse oocytes and early embryos using CARS microscopy," *Development* **143**(12) 2238–2247 (2016).
5. S. Ayyachamy and V. S. Manivannan, "Distance measures for medical image retrieval," *Int. J. Imaging Syst. Technol.* **23**(1) 9–21 (2013).
6. R. H. Wilson, K. Vishwanath, and M. Mycek, "Optical methods for quantitative and label-free sensing in living human tissues: principles, techniques, and applications," *Adv. Phys.* **1**(4), 523–543 (2016).
7. H. Segawa et al., "Multimodal imaging of living cells with multiplex coherent anti-Stokes Raman scattering (CARS), third-order sum frequency generation (TSFG) and two-photon excitation fluorescence (TPEF) using a nanosecond white-light laser source," *Anal. Sci.* **31**(4), 299–305 (2015).
8. C. L. Evans et al., "Chemical imaging of tissue in vivo with video-rate coherent anti-Stokes Raman scattering microscopy," *Proc. Natl. Acad. Sci. U. S. A.* **102**(46), 16807–16812 (2005).
9. T. Hellerer et al., "Monitoring of lipid storage in Caenorhabditis elegans using coherent anti-Stokes Raman scattering (CARS) microscopy," *Proc. Natl. Acad. Sci. U. S. A.* **104**(37), 14658–14663 (2007).

10. P. J. Campagnola et al., "High-resolution nonlinear optical imaging of live cells by second harmonic generation," *Biophys. J.* **77**(6) 3341–3349 (1999).
11. A. D. Hofemeier et al., "Label-free nonlinear optical microscopy detects early markers for osteogenic differentiation of human stem cells," *Sci. Rep.* **6**, 26716 (2016).
12. W. Min et al., "Coherent nonlinear optical imaging: beyond fluorescence microscopy," *Annu. Rev. Phys. Chem.* **62**(1), 507–530 (2011).
13. K. Svoboda and R. Yasuda, "Principles of two-photon excitation microscopy and its applications to neuroscience," *Neuron* **50**(6), 823–839 (2006).
14. H. W. Liu et al., "Molecular engineering of two-photon fluorescent probes for bioimaging applications," *Methods Appl. Fluores.* **5**(1), 012003 (2017).
15. C. Vinegoni et al., "Measurement of drug-target engagement in live cells by two-photon fluorescence anisotropy imaging," *Nat. Protoc.* **12**, 1472–1497 (2017).
16. F. Hu et al., "Bioorthogonal chemical imaging of metabolic activities in live mammalian hippocampal tissues with stimulated Raman scattering," *Sci. Rep.* **6**, 39660 (2016).
17. L. Zhang and W. Min, "Bioorthogonal chemical imaging of metabolic changes during epithelial–mesenchymal transition of cancer cells by stimulated Raman scattering microscopy," *J. Biomed. Opt.* **22**, 1–7 (2017).
18. L. Wei et al., "Vibrational imaging of newly synthesized proteins in live cells by stimulated Raman scattering microscopy," *Proc. Nat. Acad. Sci. U. S. A.* **110**(28), 11226–11231 (2013).
19. B. G. Saar et al., "Video-rate molecular imaging in vivo with stimulated Raman scattering," *Science* **330**(6009), 1368–1370 (2010).
20. M. Ji et al., "Rapid, label-free detection of brain tumors with stimulated Raman scattering microscopy," *Sci. Transl. Med.* **5**(201), 201ra119 (2013).
21. B. F. M. Romeike et al., "Coherent anti-Stokes Raman scattering and two photon excited fluorescence for neurosurgery," *Clin. Neurol. Neurosurg.* **131**, 42–46 (2015).
22. X. Li et al., "Mitochondrial imaging with combined fluorescence and stimulated Raman scattering microscopy using a probe of the aggregation-induced emission characteristic," *J. Am. Chem. Soc.* **139**(47), 17022–17030 (2017).
23. S. Awasthi et al., "Multimodal SHG-2PF imaging of microdomain Ca^{2+}-contraction coupling in live cardiac myocytes," *Circ. Res.* **118**(2), e19 (2016).
24. H. Kim et al., "Coherent Raman imaging of live muscle sarcomeres assisted by SFG microscopy," *Sci. Rep.* **7**(1), 9211 (2017).
25. J. Huang et al., "A lysosome-targetable and two-photon fluorescent probe for imaging endogenous β-galactosidase in living ovarian cancer cells," *Sens. Actuators B* **246**, 833–839 (2017).
26. F. Tian et al., "Monitoring peripheral nerve degeneration in ALS by label-free stimulated Raman scattering imaging," *Nat. Commun.* **7**, 13283 (2016).
27. L. Zhou et al., "Molecular engineering of d-A-d-based non-linearity fluorescent probe for quick detection of thiophenol in living cells and tissues," *Sens. Actuators B* **244**, 958–964 (2017).
28. H. Wang et al., "Coherent anti-Stokes Raman scattering imaging of axonal myelin in live spinal tissues," *Biophys. J.* **89**(1), 581–591 (2005).
29. H. Liu et al., "Myofibrillogenesis in live neonatal cardiomyocytes observed with hybrid two-photon excitation fluorescence-second harmonic generation microscopy," *J. Biomed. Opt.* **16**(12), 126012 (2011).
30. C. Di Napoli et al., "Quantitative spatiotemporal chemical profiling of individual lipid droplets by hyperspectral CARS microscopy in living human adipose-derived stem cells," *Anal. Chem.* **88**(7), 3677–3685 (2016).
31. M. C. Potcoava et al., "Raman and coherent anti-Stokes Raman scattering microscopy studies of changes in lipid content and composition in hormone-treated breast and prostate cancer cells," *J. Biomed. Opt.* **19**(11), 111605 (2014).
32. C. W. Freudiger et al., "Label-free biomedical imaging with high sensitivity by stimulated Raman scattering microscopy," *Science* **322**(5909), 1857–1861 (2008).
33. C. W. Freudiger et al., "Highly specific label-free molecular imaging with spectrally tailored excitation-stimulated Raman scattering (STE-SRS) microscopy," *Nat. Photonics* **5**, 103–109 (2011).

34. C. Stiebing et al., "Real-time Raman and SRS imaging of living human macrophages reveals cell-to-cell heterogeneity and dynamics of lipid uptake," *J. Biophotonics* **10**(9), 1217–1226 (2017).
35. R. Li et al., "Optical characterizations of two-dimensional materials using nonlinear optical microscopies of CARS, TPEF, and SHG," *Nanophotonics* **7**(5), 873–881 (2018).
36. W. W. Mantulin, B. R. Masters, and P. T. C. So, "Handbook of biomedical nonlinear optical microscopy," *J. Biomed. Opt.* **14**(1), 019901 (2009).
37. R. W. Boyd, *Chapter 1: The Nonlinear Optical Susceptibility, in Nonlinear Optics*, 3rd ed., Academic Press, Burlington, pp. 1–67 (2008).
38. Z. Liu et al., "A new fluorescent probe with a large turn-on signal for imaging nitroreductase in tumor cells and tissues by two-photon microscopy," *Biosens. Bioelectron.* **89**, 853–858 (2017).
39. A. V. Petukhov et al., "Energy exchange in second-order nonlinear optics in centrosymmetric media," *Phys. Status Solidi A* **170**(2), 417–422 (1999).
40. A. H. Reshak and C. R. Sheue, "Second harmonic generation imaging of the deep shade plant Selaginella erythropus using multifunctional two-photon laser scanning microscopy," *J. Microsc.* **248**(3), 234–244 (2012).
41. A. E. Hill et al., "Generation of optical harmonics," *Phys. Rev. Lett.* **7**(4), 118–119 (1961).
42. X. Chen et al., "Second harmonic generation microscopy for quantitative analysis of collagen fibrillar structure," *Nat. Protoc.* **7**, 654–669 (2012).
43. C. Macias-Romero et al., "Probing rotational and translational diffusion of nanodoublers in living cells on microsecond time scales," *Nano Lett.* **14**(5), 2552–2557 (2014).
44. S. V. Plotnikov et al., "Measurement of muscle disease by quantitative second-harmonic generation imaging," *J. Biomed. Opt.* **13**(4), 044018 (2008).
45. J. Cheng and X. S. Xie, "Coherent anti-Stokes Raman scattering microscopy: instrumentation, theory, and applications," *J. Phys. Chem. B* **108**(3), 827–840 (2004).
46. C. L. Evans and X. S. Xie, "Coherent Anti-Stokes Raman scattering microscopy: chemical imaging for biology and medicine," *Annu. Rev. Anal. Chem.* **1**(1), 883–909 (2008).
47. H. Kano et al., "Hyperspectral coherent Raman imaging: principle, theory, instrumentation, and applications to life sciences," *J. Raman Spectrosc.* **47**(1), 116–123 (2015).
48. J. Cheng et al., "An epi-detected coherent anti-Stokes raman scattering (E-CARS) microscope with high spectral resolution and high sensitivity," *J. Phys. Chem. B* **105**(7), 1277–1280 (2001).
49. J. Cheng et al., "Laser-scanning coherent anti-Stokes Raman scattering microscopy and applications to cell biology," *Biophys. J.* **83**(1), 502–509 (2002).
50. C. Krafft, B. Dietzek, and J. Popp, "Raman and CARS microspectroscopy of cells and tissues," *Analyst* **134**(6), 1046–1057 (2009).
51. M. Müller and A. Zumbusch, "Coherent anti-Stokes Raman scattering microscopy," *ChemPhysChem* **8**(15), 2156–2170 (2007).
52. K. Ishitsuka et al., "Identification of intracellular squalene in living algae, Aurantiochytrium mangrovei with hyper-spectral coherent anti-Stokes Raman microscopy using a sub-nanosecond supercontinuum laser source," *J. Raman Spectrosc.* **48**(1), 8–15 (2016).
53. R. Furuta et al., "Intracellular-molecular changes in plasma-irradiated budding yeast cells studied using multiplex coherent anti-Stokes Raman scattering microscopy," *Phys. Chem. Chem. Phys.* **19**(21) 13438–13442 (2017).
54. S. Daemen et al., "Microscopy tools for the investigation of intracellular lipid storage and dynamics," *Mol. Metab.* **5**(3), 153–163 (2016).
55. X. Chen et al., "Volumetric chemical imaging by stimulated Raman projection microscopy and tomography," *Nat. Commun.* **8**, 15117 (2017).
56. R. Long et al., "Two-color vibrational imaging of glucose metabolism using stimulated Raman scattering," *Chem. Commun.* **54**(2), 152–155 (2018).
57. W. J. Tipping et al., "Imaging drug uptake by bioorthogonal stimulated Raman scattering microscopy," *Chem. Sci.* **8**(8), 5606–5615 (2017).
58. T. Ito, Y. Obara, and K. Misawa, "Single-beam phase-modulated stimulated Raman scattering microscopy with spectrally focused detection," *J. Opt. Soc. Am. B* **34**(5), 1004–1015 (2017).

59. L. Wei et al., "Live-cell imaging of alkyne-tagged small biomolecules by stimulated Raman scattering," *Nat. Methods* **11**, 410–412 (2014).
60. X. Zhang et al., "Label-free live-cell imaging of nucleic acids using stimulated Raman scattering microscopy," *ChemPhysChem* **13**(4), 1054–1059 (2012).
61. W. Yang et al., "Simultaneous two-color stimulated Raman scattering microscopy by adding a fiber amplifier to a 2 ps OPO-based SRS microscope," *Opt. Lett.* **42**(3), 523–526 (2017).
62. L. Zhang et al., "Label-free, quantitative imaging of MoS_2-nanosheets in live cells with simultaneous stimulated Raman scattering and transient absorption microscopy," *Adv. Biosyst.* **1**(4), 1700013 (2017).
63. C. Zhang et al., "Quantification of lipid metabolism in living cells through the dynamics of lipid droplets measured by stimulated Raman scattering imaging," *Anal. Chem.* **89**(8), 4502–4507 (2017).

Rui Li received his PhD from the Department of Physics of Dalian University, China, in 2014. From 2009 to 2012, he worked as an exchanged student at the Department of Electronic Engineering, University of Texas at Arlington. Since 2014, he has worked as a lecturer at the Department of Physics of Dalian University of Technology, China. His current research interests focus on surface enhancement Raman scattering and coherent anti-stokes Raman scattering microscopy.

Xinxin Wang is the PhD candidate supervised by Professor Mengtao Sun, at the School of Mathematics and Physics, University of Science and Technology Beijing, China. Her current research interests focus on one and two photon absorptions, fluorescence, and Raman spectra.

Yi Zhou is the PhD candidate supervised by Professor Rui Li, at Dalian University of Technology. His current research interests focus on one and two photon absorptions, fluorescence, and Raman spectra.

Huan Zong is a PhD candidate supervised by Professor Mengtao Sun, at the School of Mathematics and Physics, University of Science and Technology Beijing, China. Her current research interests focus on one and two photon absorptions, fluorescence, and Raman spectra.

Maodu Chen received his PhD in 2003 from Dalian Institute of Chemical Physics, Chinese Academy of Sciences (CAS). From 2003 to 2005, he worked as a postdoc at the Department of Chemical Physics, Northwestern University. Since 2005, he has worked as an associate professor at the Department of Physics of Dalian University of Technology. In 2010, he became a full professor at Dalian University of Technology, China.

Mengtao Sun received his PhD in 2003 from the Dalian Institute of Chemical Physics, CAS. From 2003 to 2006, he worked as a postdoc at the Department of Chemical Physics, Lund University. Since 2006, he has worked as an associate professor at the Institute of Physics, CAS. In 2016, he became a full professor at the University of Science and Technology Beijing. His current research interests focus on nonlinear optical microscopy, such as CARS, TPEF, and SHG, applied in biophtonics and two-dimensional materials.